Simulation of magnetic moments in a dilute induced-moment Heisenberg magnet

1989 J. Phys.: Condens. Matter 1 6695

(http://iopscience.iop.org/0953-8984/1/37/016)

J. Phys.: Condens. Matter **1** (1989) 6695–6707. Printed in the UK

Simulation of magnetic moments in a dilute induced-moment Heisenberg magnet

Andrew Harrison
Inorganic Chemistry Laboratory, University of Oxford, South Parks Road, Oxford OX1 3QR, UK

Received 3 February 1989

Abstract. We consider a diamagnetically diluted induced-moment Heisenberg magnet in which the active sites have a singlet electronic ground state and an excited doublet state. Moments may be induced at the active sites by mixing the doublet into the singlet through a magnetic exchange interaction or an external magnetic field H_z applied parallel to the z direction. The single-ion Hamiltonian describing this system is $-\mathcal{H} = \Sigma_{ij} J_{ij} S_i S_j - \Delta \Sigma_i (S_{iz})^2 - H_z \Sigma_i S_{iz}$, where Δ is the singlet–doublet separation. Using self-consistent mean-field calculations on computer-generated lattices in one, two and three dimensions, and with connectivities $z = 2, 3, 4, 6$ and 8, we study the distribution of moments at $T = 0$ as a function of the concentration of diamagnetic impurities, the ratio J_{ij}/Δ and H. When $H_z = 0$, diamagnetic atoms rapidly reduce the value of the mean induced moment, leaving moments of significant size only in regions composed of active sites that are completely surrounded by other active sites. The sensitivity of the lattice towards dilution increases as z increases. The application of H_z compensates to some extent for the effect of the diamagnetic impurities, raising the mean moment and reducing the variance of the distribution of the size of individual moments.

1. Introduction

A dilute induced-moment magnet (IMM) is an example of a system in which there is competition between an inhomogeneous inter-site potential V_{ij} that favours order and a site-only potential V_i that disfavours order. If V_{ij} is sufficiently large relative to V_i, an order–disorder transition may be observed on warming the system from $T = 0$. For a dilute IMM, V_i is provided by a crystal-field potential that favours a non-magnetic singlet electronic ground state and V_{ij} is provided by a magnetic exchange interaction which induces a magnetic moment by mixing suitable excited electronic states into the ground state. An analogous system is provided by materials which show cooperative Jahn–Teller effects when pure and which are then diluted with Jahn–Teller inactive ions (Harley *et al* 1974). Both types of material provide testing grounds for theories that purport to describe cooperative phenomena in inhomogeneous solids.

Work on dilute IMMs has been focused on metallic alloys and most notably on the induced-moment antiferromagnet TbSb diluted with the diamagnet YSb (Cooper and Vogt 1970). There the magnetic exchange interactions have a long range and the effect of the diamagnetic dopant is satisfactorily treated using the *mean-field* approximation. Explicitly, this involves scaling the mean field linearly with the concentration of magnetic atoms. In insulating materials, in which the strength of the exchange interactions is

0953-8984/89/376695 + 13 $02.50

only significant between nearest or next-nearest neighbours, such an approximation is expected to be poor. A number of different theoretical tools have been developed to deal with such cases (Elliott *et al* 1974).

The only experimental work on diamagnetic dilution of *insulating* IMMs reported in the literature is that of Harrison and Visser (1989). In that case the pure magnet $RbFeCl_3$ contains Fe^{2+} ions whose electronic ground state is a singlet, $|m_J = 0\rangle$, with a low-lying doublet, $|m_J = \pm 1\rangle$, at an energy Δ. The superexchange interaction mixes the doublet into the singlet and is sufficiently large to induce a moment in the pure material. On doping with the diamagnet $RbMgCl_3$, T_N is found to drop more sharply than predicted by the mean-field approximation.

Chalupa *et al* (1979) showed that one consequence of the fact that the exchange interactions are very short in range in an insulator was that under certain simplifying conditions the percolative properties of such a magnet mapped onto the *bootstrap percolation* problem. They considered the case of a singlet–triplet induced-moment Ising magnet with Hamiltonian

$$-\mathcal{H} = \sum_{ij} J_{ij} S_i S_j - \Delta \sum_i S_i^2 \qquad S = -1, 0, 1 \tag{1}$$

where the magnetic exchange J_{ij} and single-ion anisotropy Δ are positive and S_i interacts with its z nearest neighbours. It was argued that to a first approximation a site could be considered to possess a magnetic moment in the magnetisation direction if m or more of its nearest neighbours also possessed a moment in that direction, where the integer m depended on the relative values of J_{ij} and Δ. In the bootstrap percolation problem the infinite cluster is made up of occupied sites that are also all connected to m or more occupied sites. This cluster is generated by first producing a lattice with a random occupancy p and then culling all sites that have fewer than m occupied nearest neighbours. If this cull is performed just once we have the *high-density percolation problem* (Reich and Leath 1978, Turban 1979, Branco *et al* 1986) and p_c is found to increase as m increases. The bootstrap percolation model is derived by repeating the culling until no more sites are vacated and the lattice is either empty or occupied only by compact clusters. As m is changed in the bootstrap percolation model, several different classes of percolation are found for two- and three-dimensional lattices of connectivity z. When m is equal to 0 or 1, 'ordinary' percolation is found and for m equal to z the 'trivial' percolation limit $p_c = 1$ is found. For intermediate values of m the geometric percolative behaviour is found either to be discontinuous (first order in p) or to show a second-order transition with critical exponents that depend on m, z and dimension d (Kogut and Leath 1981, Khan *et al* 1985, Branco *et al* 1988).

In this paper, we consider the effect of adding diamagnetic impurities to an insulating IMM with Heisenberg spin symmetry. The Hamiltonian is similar to (1) but the component of the spin in the magnetisation direction may now take a continuous range of values and it is also necessary to define the component of the spin that Δ acts on. One of the simplest examples of such a system is the singlet–doublet case described above. Thus, we shall consider the single-ion energy levels to be the same as those of Fe^{2+} in $RbFeCl_3$, where Δ is large relative to J_{ij}, acts on the z component of the spin and is positive. Consequently the moments have much larger moments in the x–y plane than along the z axis. The exchange constants will be assumed to be ferromagnetic for all the calculations, although the method is readily extended to spin arrays with a general ordering vector. The magnetisation axis is arbitrarily taken to be the x direction.

The excited doublet may also be Zeeman split by a magnetic field H applied parallel to the z direction, thereby altering the size and direction of the induced moments. So long as the applied field is not so large that the spins are pulled from the x axis to the z axis, this will compensate to some extent for the effect of dilution. The new Hamiltonian describing these interactions is then

$$-\mathcal{H} = \sum_{ij} J_{ij} S_i S_j - \Delta \sum_i (S_{iz})^2 - H_z \sum_i S_{iz} \tag{2}$$

where H_z is the component of H in the z direction. The components of the moments in the magnetisation direction have a continuous distribution rather than taking the values 0, +1 or −1 as in (1); so it is no longer possible to make the simplifying assumption that an atom only possesses a moment if there are m occupied neighbouring sites. Thus, we shall not only consider the percolative properties of such a lattice but also look at the relation between the spatial distribution of moments at $T = 0$ and the distribution of diamagnetic sites as a function of $\Sigma_{ij} J_{ij}/\Delta$, p and H_z as z is increased. The cases to be considered are $z = 3$, 4 and 6 in two dimensions (honeycomb, square and triangular lattices) and $z = 8$ in three dimensions (hexagonal lattice). These will be compared with the cases $z = 0$, 1 and 2 (isolated moments, dimers and chains) and the mean-field model. Some comparison will also be made with real systems based on $RbFeCl_3$, but a full treatment of the changes in the magnetic ordering temperature and in the neutron scattering structure factor as the concentration of diamagnetic impurities is changed awaits the extension of these calculations to finite temperatures.

2. Method

All simulations were performed in FORTRAN on a VAX cluster composed of two VAX 11/780 and two VAX 11/785 machines. One-, two- or three-dimensional lattices containing N sites were created in shapes that reflected the unit cell of the lattice to be studied—a rhombus for the honeycomb and triangular lattices, a square for the square lattice and a stack of rhombuses for the hexagonal lattice. We shall concentrate on the properties of the square lattice ($z = 4$) and also make extensive comparisons with lattices of different connectivities.

Using a random-number generator the sites were then occupied with probability p and given a uniform initial induced moment between 0.1 and 0.8. Periodic boundary conditions were employed, i.e. sites on an edge or a vertex were connected to sites on opposite edges or vertices. Each occupied site i was then taken in turn and the moment S_{ix} in the x direction calculated using Hamiltonian (1) or (2). In the absence of an applied magnetic field, S_{ix} is given by

$$S_{ix} = (2B/W)(\rho_0 - \rho_2) \tag{3}$$

in which

$$B = 2 \sum_j J_{ij} S_{jx} \tag{4}$$

$$W^2 = \Delta^2 + B^2 \tag{5}$$

and the Boltzmann factor ρ_n is given by

$$\rho_n = \exp\left(\frac{-E_n}{k_B T}\right) \Big/ \sum_m \exp\left(\frac{-E_m}{k_B T}\right) \tag{6}$$

where n and m run over the three levels of the singlet–doublet system and the eigenvalues E_n are given by

$$E_0 = \tfrac{1}{2}(\Delta - W) \tag{7}$$

$$E_1 = \Delta \tag{8}$$

$$E_2 = \tfrac{1}{2}(\Delta + W). \tag{9}$$

When a magnetic field is applied along the z axis the moment is calculated using the eigenvectors of

$$\begin{vmatrix} 0 & -B/\sqrt{2} & -B/\sqrt{2} \\ -B/\sqrt{2} & \Delta - H_z & 0 \\ -B/\sqrt{2} & 0 & \Delta + H_z \end{vmatrix}. \tag{10}$$

This was diagonalised using the NAG library routine F02ABF. For both the $H_z = 0$ and the $H_z > 0$ calculations the evaluation of the individual moments was repeated until there was a very small difference between successive values. The arbitrary value of 0.000001 spin/site was found to produce consistent results; it was ascertained that the mean moment $\langle S_{ix}\rangle_p$ per active site for a given occupancy p and given starting configuration converged to the same value regardless of the initial value taken for the moment. The mean moment $\langle S_{ix}\rangle_1$ for the pure lattice converged to the value predicted by the analytic mean-field expression.

These calculations were compared with the mean-field predictions in which the exchange field was set proportional to p. $\langle S_{ix}\rangle_p$ may be derived from (3) by setting $S_{ix} = S_{jx} = \langle S_{ix}\rangle_p$. At zero temperature this yields

$$\langle S_{ix}\rangle_p^2 = \frac{1}{p^2}\left[1 - \Delta^2 \Big/ 16\left(p\sum_j J_{ij}\right)^2\right]. \tag{11}$$

For the pure magnet ($p = 1$) the critical ratio of J_Q/Δ above which the magnetisation disappears at $T = 0$ is given by

$$R_{\text{crit}} = J_Q/\Delta = 4 \tag{12}$$

where J_Q is the total exchange field in the ordered ground-state spin configuration. In the present set of simulations, we mainly use values of J_Q/Δ that are 1% and 2% greater than R_{crit}, i.e. $J_Q/\Delta = 1.01R_{\text{crit}}$ and $1.02R_{\text{crit}}$ respectively.

The cases $z = 0$ and $z = 1$ on an infinite lattice have simple exact solutions for the magnetisation as a function of p:

$$z = 0 \qquad \langle S_{ix}\rangle_p/\langle S_{ix}\rangle_1 = 1 \tag{13}$$

$$z = 1 \qquad \langle S_{ix}\rangle_p/\langle S_{ix}\rangle_1 = p. \tag{14}$$

3. Results and discussion

3.1. $H_z = 0$, $T = 0$

The results of simulations for $z = 2$ ($d = 1$), $z = 3, 4, 6$ ($d = 2$) and $z = 8$ ($d = 3$) showed fluctuations in $\langle S_{ix}\rangle_p/\langle S_{ix}\rangle_1$ at a given value of p owing to the influence of different

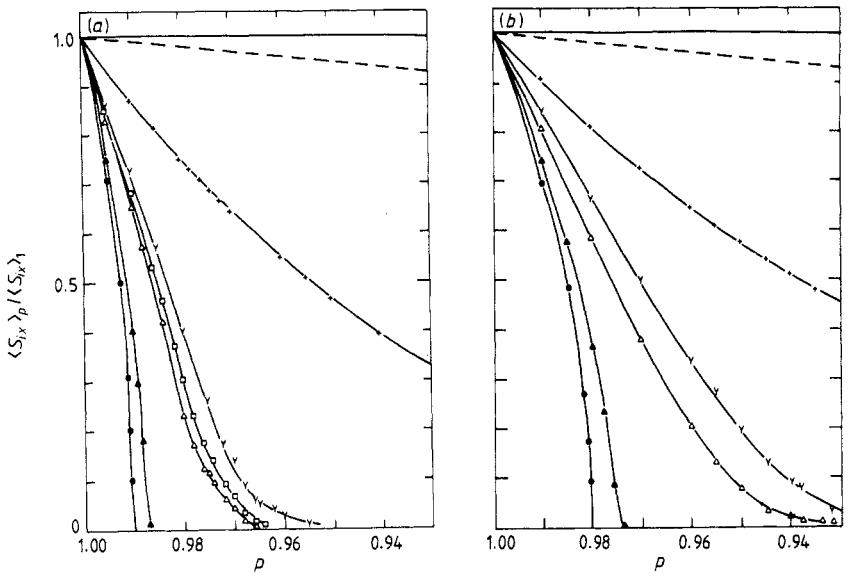

Figure 1. The dependence of the mean magnetic moment $\langle S_{ix}\rangle_p/\langle S_{ix}\rangle_1$ in the x direction on the connectivity z and occupancy p of active sites in a lattice of size $N = 10^4$ at a temperature $T = 0$ for (*a*) $J_Q/\Delta = 1.01R_{crit}$ and (*b*) $J_Q/\Delta = 1.02R_{crit}$. ——, $z = 0$; – – – –, $z = 1$; +, $z = 2$, $d = 2$; Y, $z = 3$, $d = 2$; □, $z = 4$, $d = 2$; △, $z = 6$, $d = 2$; ▲, $z = 8$, $d = 3$; ●, the mean-field case.

starting configurations on the behaviour of a finite sample. These fluctuations were most pronounced at lower values of N, p and z. Thus, we display results for the largest lattices considered ($N = 10^4$), averaging over three to five starting configurations for each value of p. Figures 1(*a*) and 1(*b*) demonstrate the reduction in $\langle S_x\rangle_p/\langle S_x\rangle_1$ as p is reduced for $J_Q/\Delta = 1.01R_{crit}$ and $1.02R_{crit}$ respectively. These curves change in a regular fashion with z between the known limits $z = 1$ and the mean-field case. They involve an average over all active sites and do not provide much information about the distribution of moments in the various lattices. Let us consider the influence of the diamagnetic sites on the distribution of the moments at a microscopic level.

In the linear case ($z = 2$) it is clear that a pair of diamagnetic impurities at a given separation create a void between them if J_Q/Δ lies below some critical value (we define a void as a region composed of diamagnetic sites or active sites with *zero* induced moment). Conversely, for a fixed value of J_Q/Δ there is a critical size above which clusters of finite induced moments are stable. In two- and three-dimensional arrays a similar criterion exists for the formation of voids. Such regions have to be separated from the infinite percolating cluster by diamagnetic sites and they must be smaller than a critical size that depends on the ratio J_Q/Δ and on the perimeter or surface area of the cluster of active sites.

The induced-moment character of the active sites also has a profound effect on the percolating cluster. Let us first consider the case where p is low and then the case where p approaches p_c, the ordinary percolation threshold for site dilution of the appropriate lattice. Figures 2(*a*)–2(*d*) illustrate the spatial distribution of the individual moments $(S_{ix})_p$ for square lattices with occupancies $p = 0.99$, 0.98, 0.97 and 0.96, respectively and $J_Q/\Delta = 1.02R_{crit}$. When $p = 0.99$, regions where impurities lie close together are

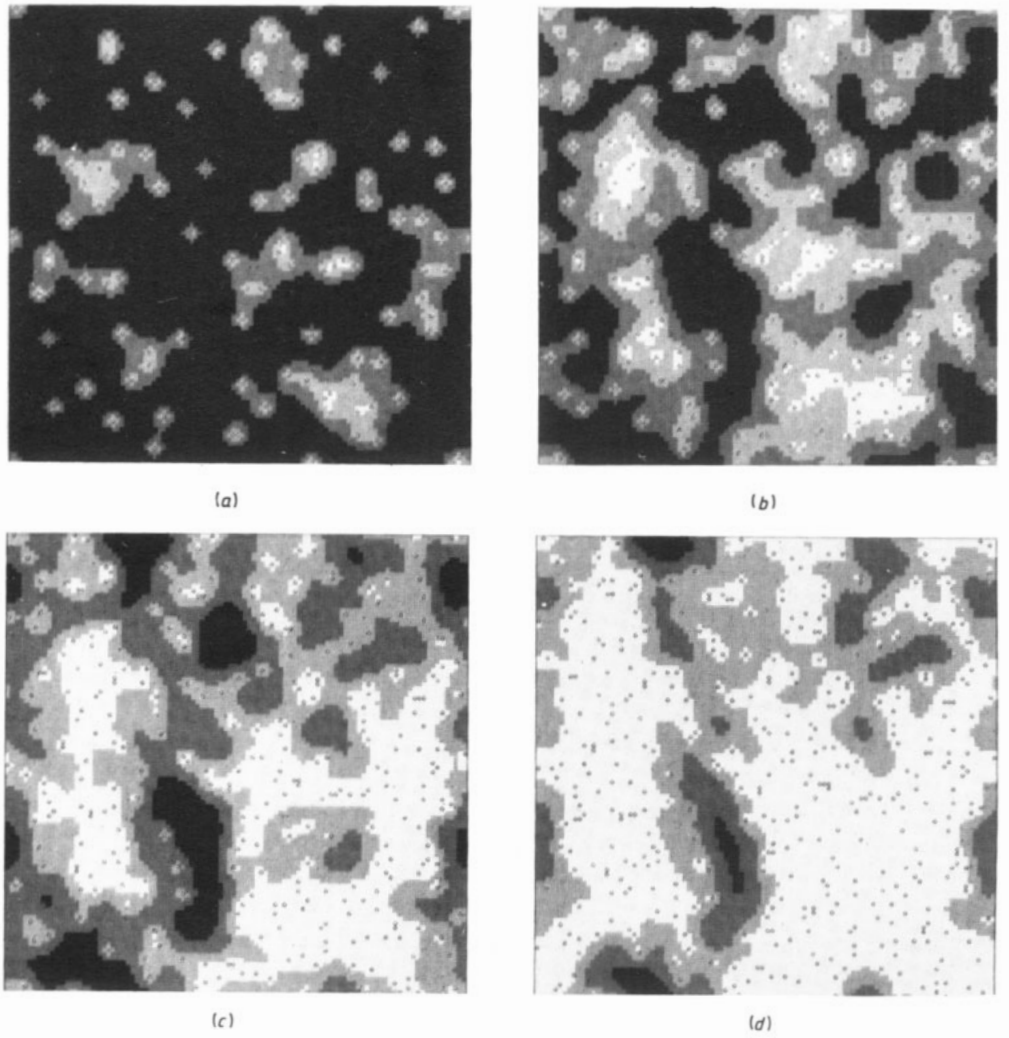

Figure 2. The distribution of induced moments on square lattices of size $N = 10^4$ containing active sites with $J_Q/\Delta = 1.02R_{crit}$ for occupancies of (*a*) 0.99, (*b*) 0.98, (*c*) 0.97 and (*d*) 0.96. The size of the induced moment at each site is expressed as a fraction of the moment $\langle S_{\alpha}\rangle_1$ in the corresponding pure magnet and denoted by one of four grey tones. The lightest shade corresponds to (0.00–0.25) $\langle S_{\alpha}\rangle_1$ and the darkest to (0.75–1.00) $\langle S_{\alpha}\rangle_1$.

Figure 3 (opposite). The distribution of induced moments on (*a*), (*d*) honeycomb, (*b*), (*e*) square and (*c*,) (*f*) triangular lattices of the same size ($N = 10^4$), occupancy ($p = 0.96$), configuration of diamagnetic impurities and $J_Q/\Delta = 1.02R_{crit}$. The honeycomb and triangular lattices have been distorted to adopt a square shape and the individual cells for (*a*), (*d*), (*b*), (*e*) and (*c*), (*f*) have the connectivity maps

(*a*), (*d*)  (*b*), (*e*)  (*c*), (*f*) 

(*a*)–(*c*) illustrate the distribution of sizes of induced moments using the same shading scale as figure 2. (*d*)–(*f*) show the effect of five successive cycles of culling sites with fewer than z nearest-neighbour active sites. The remaining active sites are black.

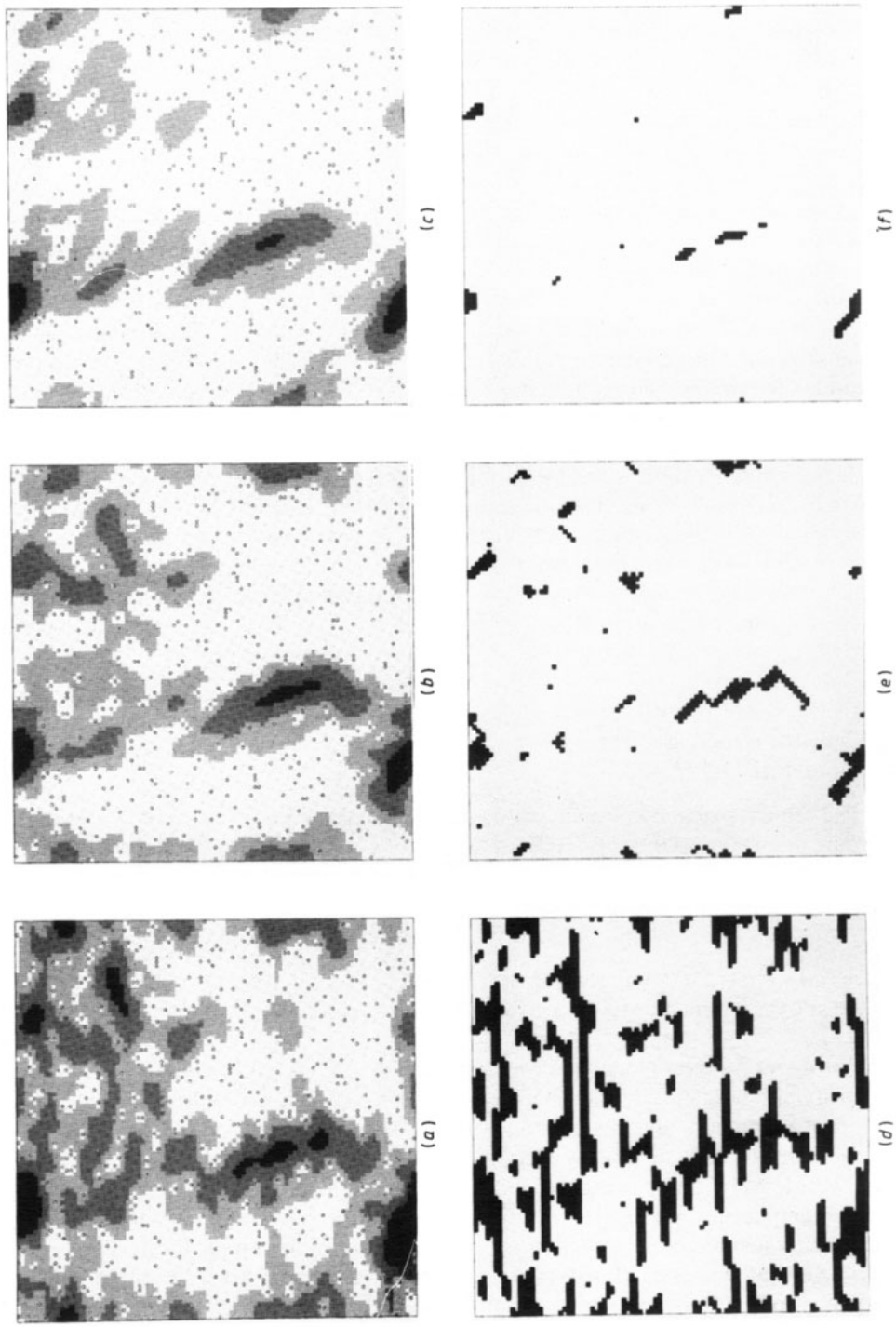
(c)
(f)
(b)
(e)
(a)
(d)

distinguished by the large depletion of moments on neighbouring active sites—'*giant holes*' are created. At $p = 0.96$, we observe the formation of islands of active sites with moments similar to those in the pure magnet, surrounded by a sea of diamagnetic sites and active sites with very small moments. The islands contain a high proportion of active sites with maximum local exchange interactions, i.e. active sites with all z neighbouring sites also occupied by active sites. We call this *coordination saturation*. In figures 3(*a*)–3(*c*) we compare the distribution of induced moments on honeycomb, square and triangular lattices, respectively, with identical configurations of diamagnetic impurities, occupancy $p = 0.96$ and $J_Q/\Delta = 1.02R_{\text{crit}}$. It is clear that, as z increases, $\langle S_{ix}\rangle_p$ decreases and the size of the islands of relatively large induced moments also gets smaller.

When p approaches p_c, it is helpful to consider the structure of the infinite cluster in terms of the 'nodes–links–blobs' picture (Coniglio 1982, 1983, de Jongh *et al* 1985). As defined originally, this model refers to the bond dilution case, and we refer to it here merely to describe the general structure of the infinite cluster near p_c. The infinite cluster is then envisaged as being constructed from three types of building unit: *links* are made up of bonds such that, if one of these bonds is cut, the cluster is broken into two pieces; *nodes* are the intersections of links; *blobs* are regions of high bond density and are not divided into two pieces just by cutting one bond. Blobs may also be nodes and at p_c are themselves composed of links and blobs in a self-similar fashion. Some of the blobs will contain very large collections of atoms with coordination saturation—so large that they would survive if they were isolated finite clusters. These regions will act on surrounding active sites in the nodes and links and in the smaller blobs, inducing moments at those sites. Although the exchange field will attenuate rapidly away from such large blobs, all the moments in the percolating cluster will be finite. The persistence of relatively large moments in the large blobs gives rise to the tails in the plot of $\langle S_{ix}\rangle_p/\langle S_{ix}\rangle_1$ against p (figure 1).

Thus, there are several aspects of the distribution of moments that change systematically as z is increased for a given value of d and a given starting configuration at zero temperature and $H_z = 0$.

(i) The critical size above which a finite cluster may survive is increased.

(ii) The resistance to the formation of 'giant holes' or regions of greatly diminished moments near high concentrations of diamagnetic sites decreases.

(iii) The regions containing relatively large moments in the large blobs are reduced in size.

These all stem from the increasing difficulty of producing regions of coordinatively saturated sites as z is increased for a given occupancy p and distribution of diamagnetic sites.

Our problem is not as cleanly defined as correlated percolation models such as the high-density and bootstrap models because the sites that have coordination $m < z$ still possess finite moments and are therefore still part of some cluster. However, some similarity might be expected between the structure of clusters in the high-density percolation problem and the shape of the regions of frozen moments at finite temperatures.

As the temperature is raised from zero, the ordered array of moments in the nodes and links and smaller blobs will rapidly melt, leaving moments in the larger blobs frozen in superparamagnetic clusters. In figures 3(*d*)–3(*f*), we illustrate the effect of successively culling sites with fewer than three, four or six nearest neighbours on honeycomb, square and triangular lattices, respectively. The occupancy p and configuration of diamagnetic sites are identical with those in figures 3(*a*)–3(*c*) and we display

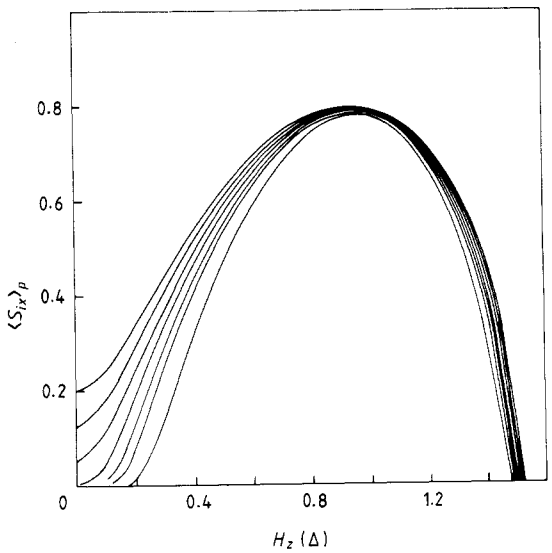

Figure 4. The dependence on magnetic field H_z applied parallel to the z axis and occupancy p of active sites of $\langle S_{ix}\rangle_p$ for the square lattice of size $N = 10^4$, with $J_Q/\Delta = 1.02R_{crit}$. The different curves apply to the values $p = 1.00, 0.98, 0.96, 0.94, 0.92, 0.90$ and 0.85, decreasing in height as p decreases.

the result of five successive culls. The remaining active sites adopt patterns that resemble the regions with the largest moments in figures 3(*a*)–3(*c*). Differences betwen the two sets of figures are also apparent. These reflect the fact that the culling is a sequential nearest-neighbour process and fails to mimic the long-range influence of impurity centres in the simulations, reaching beyond the current position of the culling front.

3.2. $H_z > 0$, $T = 0$

There are two principal changes seen in $\langle S_{ix}\rangle_p/\langle S_{ix}\rangle_1$ when a magnetic field is applied along the z axis.

(i) $\langle S_{ix}\rangle_p/\langle S_{ix}\rangle_1$ rises with H_z until $H_z = \Delta$ and then falls to zero as the moments are pulled towards the z axis (figure 4). Thus, moments may be induced in dilute materials that show no moment in zero field.

(ii) Curves of $\langle S_{ix}\rangle_p/\langle S_{ix}\rangle_1$ drawn for the same value of J_Q/Δ and different values of p almost converge at $H_z = \Delta$ (figure 4). This implies that the values of individual moments may also tend to very similar values as H_z is increased. Figures 5(*a*)–5(*c*) show the distribution of individual moment values $(S_{ix})_p$ as a function of p and H_z for the square lattice. Figures 6(*a*)–6(*c*), showing the distribution for linear, honeycomb and triangular lattices with occupancy $p = 0.96$, should be compared with figure 5(*c*) to show the effect of changing z. Thus, for $p = 0.96$ on all the two-dimensional lattices shown the moments are small and adopt a broad distribution in low magnetic fields. At higher values of H_z, two peaks are distinguishable. As H_z is increased to Δ, the centres of these peaks become very close. Scrutiny of the spatial distribution of the moments reveals that the smaller of the two peaks at lower values of $(S_{ix})_p$ corresponds to active sites adjacent to diamagnetic impurities.

This result is consistent with some of the conclusions drawn from neutron scattering measurements on $RbFeCl_3$ doped with the isomorphous compound $CsFeCl_3$ (Harrison *et al* 1986). Pure $CsFeCl_3$ has a similar electronic structure to $RbFeCl_3$, but the ratio J_Q/Δ is now too small for a moment to be induced. On doping Cs^+ ions into $RbFeCl_3$,

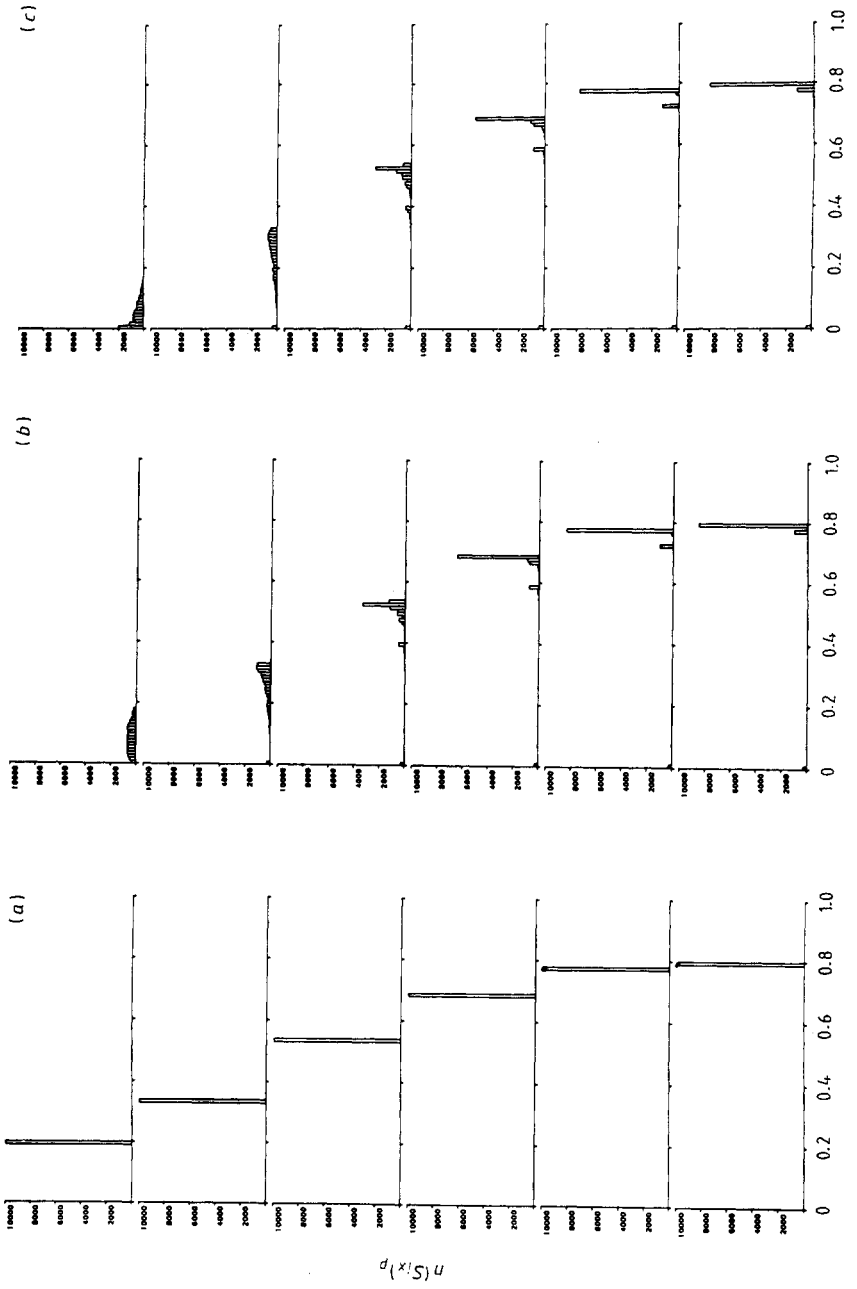

Figure 5. The distribution of individual magnetic moments $(S_\alpha)_p$ in the x direction for a square lattice of size $N = 10^4$ for occupancies p of (*a*) 1.00, (*b*) 0.98 and (*c*) 0.96 and for magnetic fields H_z of (i) 0, (ii) 0.2Δ, (iii) 0.4Δ, (iv) 0.6Δ, (v) 0.8Δ and (vi) Δ. In each case the distribution is given on a linear scale from 0 to 10000.

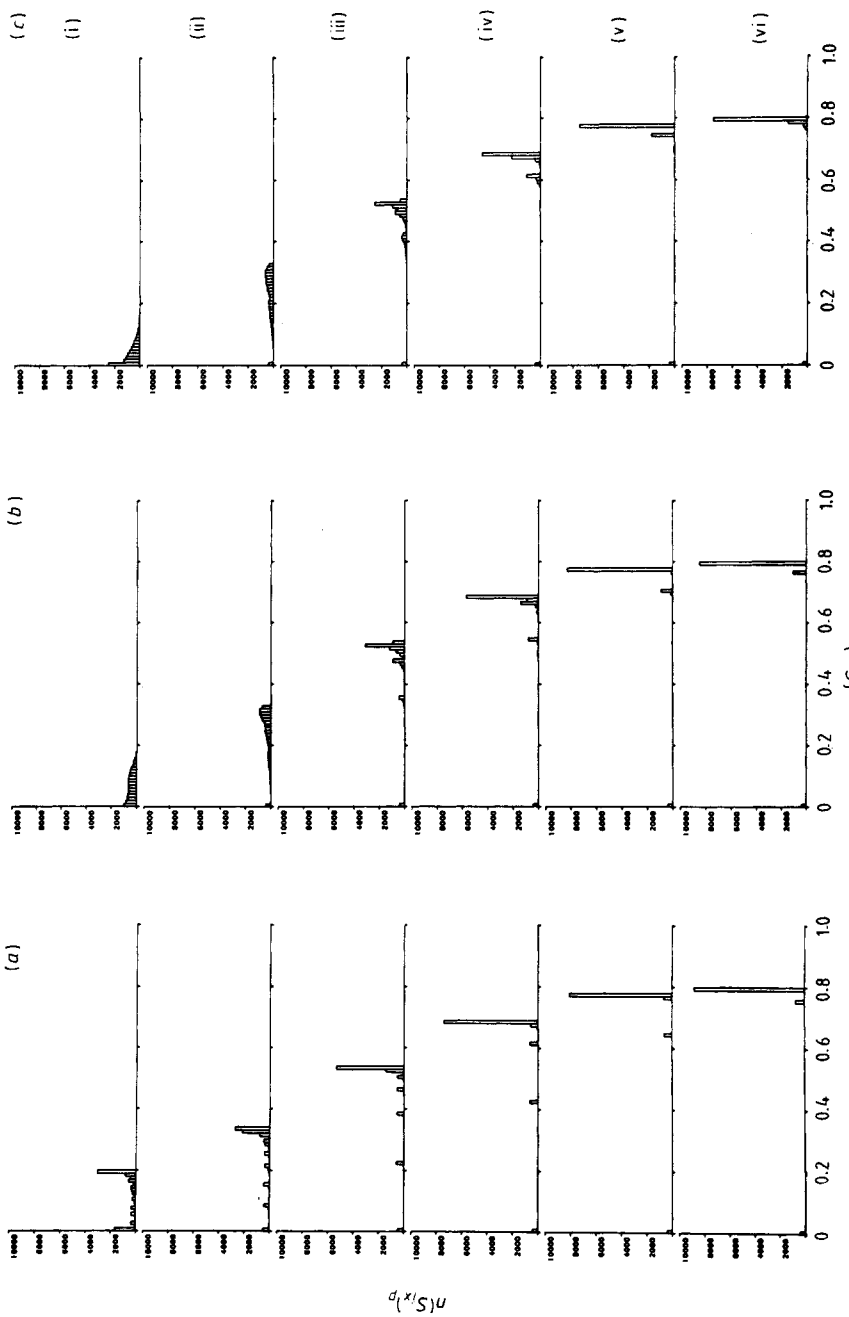

Figure 6. The distribution of individual magnetic moments $(S_\alpha)_p$ in the x direction for (*a*) linear ($z = 2$), (*b*) honeycomb ($z = 3$) and (*c*) triangular ($z = 6$) lattices of size $N = 10^4$, occupancy $p = 0.96$ and magnetic fields H_z of (i) 0, (ii) 0.2Δ, (iii) 0.4Δ, (iv) 0.6Δ, (v) 0.8Δ and (vi) Δ. In each case the distribution is given on a linear scale from 0 to 10000.

local structural distortions are introduced that reduce the value of J_Q/Δ for neighbouring Fe^{2+} ions. Small amounts of $CsFeCl_3$ (less than 5%) destroy the magnetic long-range order seen in pure $RbFeCl_3$. The magnetic order may be restored to some extent by applying a magnetic field parallel to the crystal c axis. As H_z is increased, the magnetic ordering temperature increases and the degree of magnetic inhomogeneity, measured in terms of the width of magnetically scattered neutron diffraction peaks, decreases.

4. Conclusions

The present set of simulations demonstrate that the distribution of moments in a dilute induced-moment magnet at $T = 0$ with nearest-neighbour magnetic exchange and Heisenberg spin symmetry does not map onto the bootstrap percolation problem. Although the size of an induced moment is greatly reduced when the number of nearest-neighbour active sites is reduced, it remains finite so long as it is connected to regions of the lattice with a high density of coordinatively saturated sites. However, as the temperature is raised from zero and the ordered arrays of smaller moments melt, the regions of larger frozen moments should adopt shapes that resemble the active sites that remain after several culling cycles of the bootstrap percolation model.

There is a need to extend this work to finite temperatures, performing Monte Carlo simulations to show how $\langle S_{ix} \rangle_p$ changes with temperature, and how thermodynamic variables such as the heat capacity and magnetic susceptibiltiy depend on p, J_Q/Δ and lattice type. There is also much scope for experimental work, applying neutron diffraction techniques to dilute insulating Heisenberg induced-moment magnets to measure the distribution of the size and position of moments as a function of H_z and T. Materials basded on $RbFeCl_3$ or $RbFeBr_3$ are not ideal for this purpose because they contain a triangular antiferromagnetic spin array in their magnetically ordered ground state, and the frustration inherent in such an array will complicate the ordering processes in the dilute materials. However, the data available to date on diamagnetically diluted samples of these materials have revealed a general correspondence to the results of the simulations presented here.

Acknowledgments

The author is grateful to Dr J M F Gunn (Rutherford Appleton Laboratory, UK) for drawing his attention to correlated percolation problems, and to Dr R B Stinchcombe (Department of Theoretical Physics, University of Oxford) for pointing out the work of Harley *et al* (1974). Finally, he thanks St John's College, University of Oxford, for financial support. He is grateful to the staff of the Oxford University Computing Service for their assistance with figures 2 and 3, and in particular to Malcolm Austen.

References

Branco N S, de Queiroz S L A and dos Santos R R 1986 *J. Phys. C: Solid State Phys.* **19** 1909
—— 1988 *J. Phys. C: Solid State Phys.* **21** 2463
Chalupa J, Leath P L and Reich G R 1979 *J. Phys. C: Solid State Phys.* **12** L31
Coniglio A 1982 *J. Phys. A: Math. Gen.* **15** 3829
—— 1983 *Magnetic Phase Transitions* ed. M Ausloos and R J Elliott (Berlin: Springer) p 195

Cooper B R and Vogt O 1979 *Phys. Rev.* B **1** 1218
de Jongh L J, Mennenga G and Coniglio A 1985 *Physica* B **132** 100
Elliott R J, Krumhansl J A and Leath P L 1974 *Rev. Mod. Phys.* **46** 465
Harley R T, Hayes W, Perry A M, Smith S R P, Elliott R J and Saville I D 1974 *J. Phys. C: Solid State Phys.* **7** 3145
Harrison A and Visser D 1989 *J. Phys.: Condens. Matter* submitted
Harrison A, Visser D, Day P, Knop W and Steiner M 1986 *J. Phys. C: Solid State Phys.* **19** 6811
Khan M A, Gould H and Chalupa J 1985 *J. Phys. C: Solid State Phys.* **18** L223
Kogut P M and Leath P L 1981 *J. Phys. C: Solid State Phys.* **14** 3187
Reich G R and Leath P L 1978 *J. Stat. Phys.* **19** 611
Turban L 1979 *J. Phys. C: Solid State Phys.* **12** 5009